Turkish Journal of Earth Sciences (Turkish J. Earth Sci.), Vol. 21, 2012, pp. 1029–1045. 
doi:10.3906/yer-1005-15 First published online 22 February 2011

# Petrogenesis of Late Cretaceous Adakitic Magmatism in the İstanbul Zone (Çavuşbaşı Granodiorite, NW Turkey)

SABAH YILMAZ ŞAHİN, NAMIK AYSAL & YILDIRIM GÜNGÖR

İstanbul University, Engineering Faculty, Department of Geological Enginering, Avcılar, TR−34320 İstanbul, Turkey (E-mail: sabahys@istanbul.edu.tr)

*Received 15 May 2010; revised typescripts received 31 January 2011 & 21 February 2011; accepted 22 February 2011*

**Abstract:** The Çavuşbaşı granodiorite intrudes Ordovician sedimentary rocks in the western part of the İstanbul Zone (NW Turkey). The intrusion is made up mainly of granodiorite, and subordinate tonalite and quartz diorite, and has a granular texture and some special mixing textures such as antirapakivi, blade-shaped biotite, acicular apatite, spongy cellular dissolution/melting plagioclase textures. The main mafic minerals are hornblende and biotite. U-Pb in-situ dating of zircons from two samples via SHRIMP yielded weighted age values of ~68 Ma, suggesting emplacement during the Late Cretaceous. Geochemically the Çavuşbaşı granodiorite resembles adakites with high Sr/Y and La/Yb ratios, low Y and HREE contents and no Eu anomaly. It contains 63.4 (wt%) >$SiO_2$, and is I-type, metaluminous, middle-K calc-alkaline. These adakitic rocks have high values of MgO (0.77–2.56 wt%), Mg# (45.3–59.3) and LILE (e.g., Rb, K, Ba, Sr). Initial εNd and $^{87}Sr/^{86}Sr$ values are 3.2–3.7 and 0.7035–0.7036, respectively. Based on the continuing subduction along the İzmir-Ankara and Intra-Pontide Neo-Tethyan oceanic domains and depleted Sr-Nd isotopic signatures, we suggest that the adakitic magmas may be derived from the partial melting of an oceanic slab under amphibole-eclogite facies conditions.

**Key Words:** İstanbul Zone, adakite, SHRIMP dating, Sr-Nd isotops, arc-related, slab melting, Neo-Tethyan Ocean

## İstanbul Zonu'ndaki Geç Kretase Yaşlı Adakitik Magmatizmanın Petrojenezi (Çavuşbaşı Granodiyoriti, KB Türkiye)

**Özet:** Çavuşbaşı granodiyoriti, İstanbul Zonu'nun (KB Türkiye) batısında yer alır ve Ordovisyen yaşlı sedimanter kayaçlar içerisine sokulum yapar. İntrüzyon, başlıca, granodiyorit, seyrek olarak da tonalit ve kuvars diyorit bileşimindedir. Granitik kayaçlar genellikle tanesel dokuludur ve antirapakivi, bıçağımsı biyotit, iğnemsi apatit ve plajiyoklazlarda süngerimsi hücreli çözünme/erime dokuları gibi bazı özel '*mixing*' dokuları da gösterirler. Ana mafik mineraller hornblend ve biyotittir. Birime ait iki örneğin zirkon minerallerinde yapılan SHRIMP U-Pb yaşlandırmasında ~68 My yaşı elde edilmiş olup, plütonun Geç Kretase döneminde sokulum yaptığını göstermektedir. Çavuşbaşı granodiyoriti jeokimyasal olarak, yüksek Sr/Y ve La/Yb oranları ile düşük Y, HREE ve Eu anomalisinin olmaması ile adakitik kayaçlara benzemektedir. Plüton %63.4 >$SiO_2$ içeren, I-tipi, metalüminolu, orta-K'lu, kalk-alkalin özelliklere sahiptir. Bu adakitik kayaçlar yüksek MgO (% 0.77–2.56 ağırlık), Mg# (45.3–59.3), LIL (Rb, K, Ba, Sr, vb.) element oranlarını içerir. İlksel εNd ve $^{87}Sr/^{86}Sr$ oranları sırasıyla 3.2–3.7 ve 0.7035–0.7036' dır. Neo-Tetis okyanusunun kuzey kolunun kapanmasıyla ilgili İzmir-Ankara-Erzincan ve Intra-Pontid sütürları boyunca var olan dalma-batma olayının varlığı temel alındığında, adakitik magmaların dalan okyanusal dilimin amfibol-eklojit fasiyesi koşulları altında kısmi erimesi ile oluşmuş olabileceği ileri sürülebilir.

**Anahtar Sözcükler:** İstanbul Zonu, adakit, SHRIMP yaşlandırma, Sr-Nd izotopları, yayla ilgili, ergiyen dilim, Neo-Tetis Okyanusu

## Introduction

Arc magmatism orginates from the partial melting of a peridotitic mantle wedge, induced by generation of fluids released from the subducting slab in convergent margins (e.g., Davies & Stevenson 1992; Chiaradia 2009). Another rock type associated with convergent margins is adakite, which is produced by melting of basaltic materials under garnet-stable conditions in their source region, characterized by high Sr/Y and La/Yb ratios (e.g., Martin 1999). However, not all adakitic magmas are generated by the melting of the subducting slab. Models proposed for the generation of adakitic magmas include (i) partial melting of subducted oceanic slab (Defant & Drummond 1990;

Defant *et al*. 1991); (ii) partial melting of thickened mafic lower crust (Atherton & Petford 1993; Castillo *et al.* 1999; Castillo 2006; Chiaradia 2009) and Archaean tonalite-trondhjemite-granodiorite (TTG) (Smithies & Champion 2000; Smithies *et al.* 2003; Condie 2005), and (iii) high-pressure fractionation of mantle-wedge derived magmas (Castillo *et al.* 1999; Macpherson *et al.* 2006). Understanding the origin of modern adakites is important for the evolution of continental crust. Although the term 'adakite' is traditionally used for volcanic rocks (Defant & Drummond 1990; Le Maitre *et al.* 2002), many plutonic equivalents are genetically similar to adakite (e.g., Martin 1999; Martin *et al.* 2005).

Late Cretaceous arc magmatism is widespread throughout the Pontides. The products of arc magmatism are currently defined as the classical arc type based on some geochemical features. The arc magmatism is ascribed to the north-vergent subduction of the Neo-Tethyan ocean along the İzmir-Ankara-Erzincan suture (Pecerillo & Taylor 1976; Şengör & Yılmaz 1981; Yeniyol & Ercan 1989-1990; S. Yılmaz & Boztuğ 1996; Y. Yılmaz *et al.* 1997; Okay & Şahintürk 1997; Okay & Tüysüz 1999; Yılmaz Şahin *et al.* 2004; Yılmaz Şahin 2005; Keskin *et al.* 2003, 2010). In this paper, we describe for the first time adakitic magmatism of Late Cretaceous age, the Çavuşbaşı granodiorite, from the western Pontides, present field, geological, geochemical and geochronological data, and discuss it in terms of the geodynamic framework. Post-collisonal Early Eocene and Miocene adakitic magmatism is described from the Eastern Pontides, Central Anatolia and the Anatolide-Tauride Belt (Topuz et *al.* 2005, 2011; Varol *et al.* 2007; Kadıoğlu & Dilek 2010; Karslı *et al.* 2010). In addition, there are Upper Palaeocene–Lower Eocene (55 Ma) adakitic rocks (Kop Mountain area) in eastern Pontides arc, generated by a slab window processes in a subduction-related setting (Eyüboğlu *et al.* 2011).

## Geological Setting

The Pontides (Northern Turkey) comprise the Strandja, İstanbul and Sakarya zones (Ketin 1966; Okay & Tüysüz 1999; Figure 1a). The İstanbul Zone includes Ordovician to Carboniferous sedimentary successions on Proterozoic basement metamorphic rocks and granitoids (Ustaömer & Rogers 1999; Yiğitbaş *et al.* 1999, 2004; Chen *et al.* 2002; Okay *et al.* 2008). In the western part of İstanbul Zone, granitoids of two different ages are present: the Permian Sancaktepe granite and the Late Cretaceous Çavuşbaşı granodiorite (Ketin 1941; Abdüsselâmoğlu 1963; Bürküt 1966; Öztunalı & Satır 1973, 1975; I. Yılmaz 1977; Ketin 1983; Yılmaz Şahin *et al.* 2009, 2010; Figure 1a). In addition, there are volcanic equivalents of the Upper Cretaceous Çavuşbaşı granodiorite in the northern part of İstanbul city along the Black Sea coast (Keskin *et al.* 2003).

The Çavuşbaşı granodiorite is highly weathered, and covered by a 20–25-m-thick regolith. Fresh outcrops are found in stream valleys. It intrudes Ordovician arkosic sandstones (Kurtköy Formation) and has an overall ellipsoidal shape with a well-developed contact metamorphic aureole (Ketin 1941; Figure 1b). The arkosic sandstones were converted into hornfelses within the contact aureole (Figure 1b). The pluton is cut by dykes of dacite, andesite, aplite and microdiorite up to ~5 m thick, striking mostly NW–SE and NE–SW (Figure 2a). The main body of the pluton is cut by aplite and microdiorite and the surrounding Ordovician series is cut by dacitic and andesitic dykes. The youngest dykes are microdioritic. The dykes cannot be followed long distances along strike; and are lost after a few metres due to lack of outcrops or deformation. The pluton locally contains mafic magmatic enclaves (MME; Figure 2b) that formed as the result of mingling of coeval felsic and mafic magmas (cf. Didier & Barbarin 1991; Barbarin & Didier 1992). The lengths of the mafic enclaves range from 3–5 to 50 cm. Mafic microgranular enclaves are ovoid-ellipsoidal, fine-grained, dark and monzodioritic in composition. They have gradational boundaries with the host rock (Figure 2b) and generally consist of plagioclase, rare K-feldspar, quartz, amphibole and biotite.

## Analytical Tecniques

In this work, ten granitic samples for geochemical analyses, two samples for isotope geochemistry, two samples for SHRIMP-II (Sensitive High Resolution Ion Microprobe) zircon U-Pb and one sample for K-Ar geochronological determination were chosen from the Çavuşbaşı pluton.

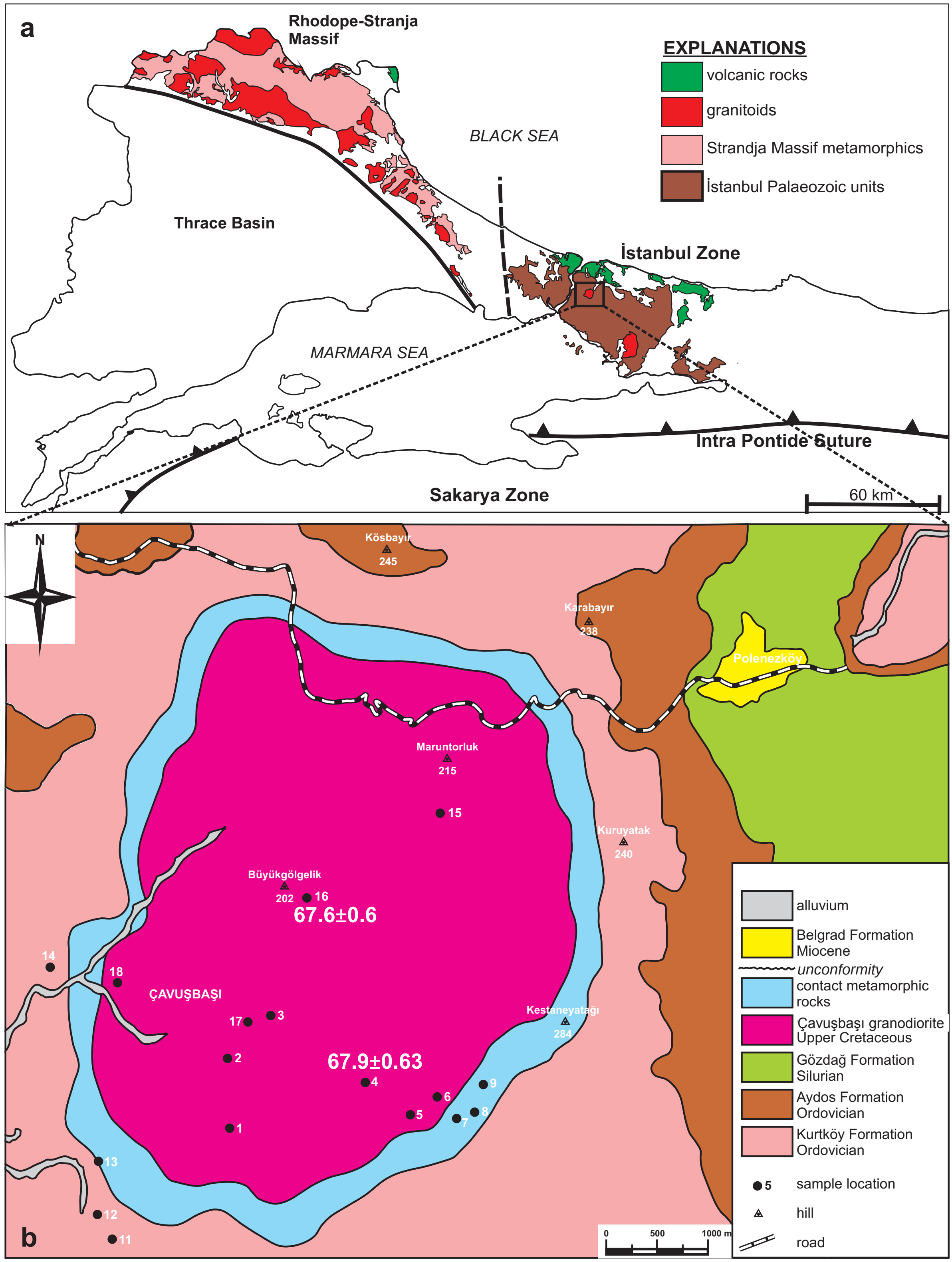


**Figure 1.** **(a)** Location map of the studied area (taken from MTA 1/500.000 scale map; suture zones from Okay & Tüysüz 1999), **(b)** Geological map of the Çavuşbaşı granodiorite (Ketin 1941).

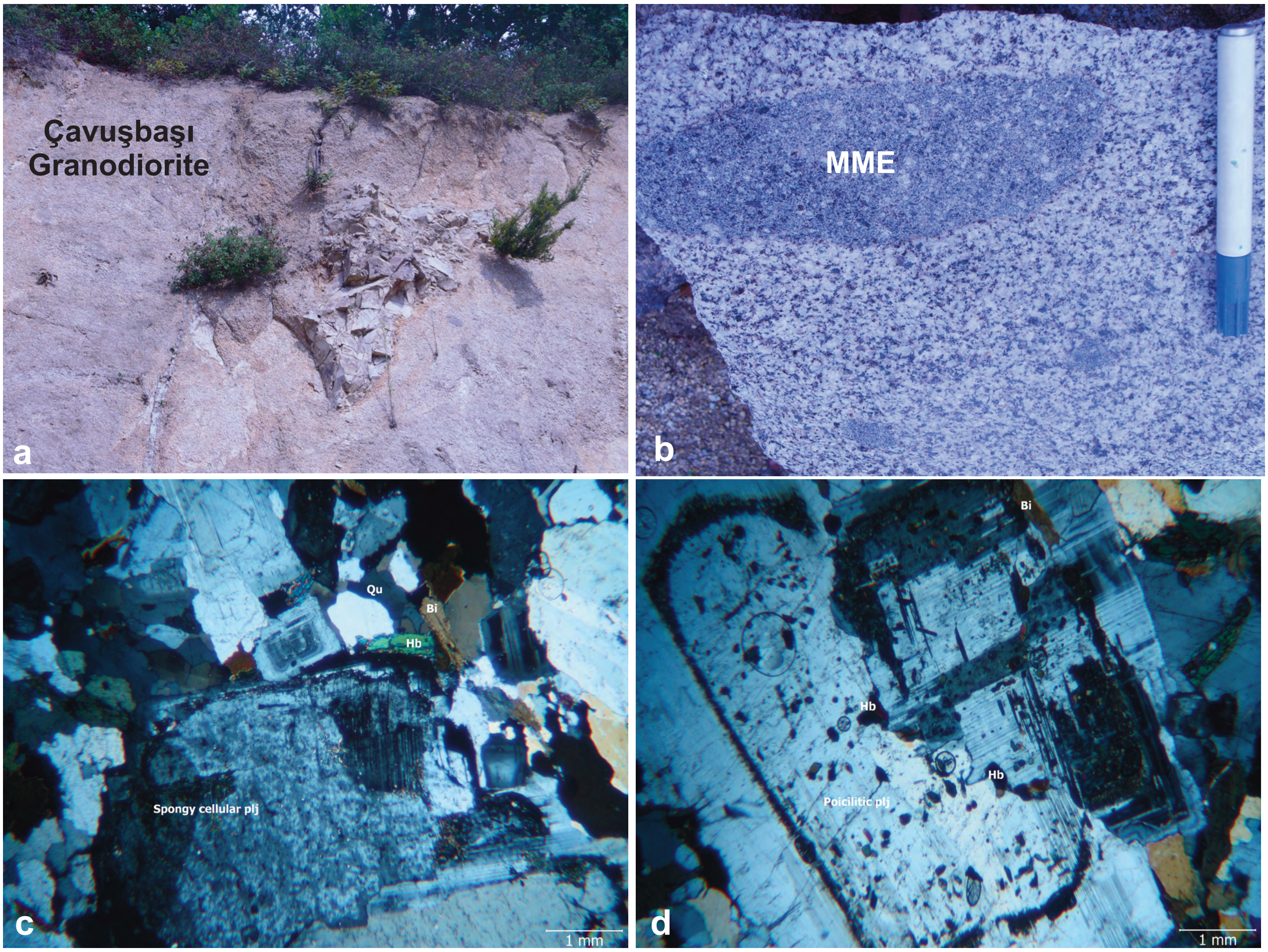


**Figure 2.** **(a)** Altered outcrop of the Çavuşbaşı granodiorite; **(b)** Mafic microgranular enclaves (MME) in the Çavuşbaşı granodiorite; **(c)** Spongy cellular dissolution/melting texture in plagioclase, **(d)** Poikilitic feldspar texture from mixing textures (Hibbard 1991) in the Çavuşbaşı granodiorite.

Whole rock analyses of major and trace elements were determined by ICP-emission spectrometry and ICP-mass spectrometry using standard techniques at ACME, Analytical Laboratories Ltd., Vancouver (Canada). 0.2 g of rock-powder was fused with 1.5 g $LiBO_2$ and dissolved in 100 ml 5% $HNO_3$. Loss on ignition (LOI) was determined on dried samples heated to a temperature of 1000°C. REE analyses were performed by ICP-MS at ACME. Detection limits ranged from 0.01 to 0.1 wt% for major oxides, from 0.1 to 10 ppm for trace elements, and from 0.01 to 0.5 ppm for REE (Table 1).

For the radiometric age dating, heavy minerals were seperated from Çavuşbaşı granodiorite rocks using heavy liquids after crushing, grinding, sieving and cleaning. Zircons were extracted from ~5 kg fresh rocks. Approximately 100 zircon grains were seen from each sample under a binocular microscope. The selected zircon grains were placed on double-sided tape, mounted in epoxy together with chips of the reference zircons (Temora, and SL13), sectioned approximately in half, and polished. Reflected and transmitted light photomicrographs were prepared for all zircons, as were cathodoluminescence (CL) and scanning electron microscope (SEM) images (Figure 3). These CL images were used to decipher the internal structures of the sectioned grains and to ensure that the ~20 µm SHRIMP spot was wholly within a single age component within the sectioned grains.

**Table 1.** Whole-rock major (wt%), trace (ppm) and rare earth elements (REE) (ppb) geochemical data from the Çavuşbaşı granodiorite.

| | CG-1 | CG-2 | CG-4 | CG-6 | CG-7 | CG-12 | CG-15 | CG-16 | CG-17 | CG-18 |
|---|---|---|---|---|---|---|---|---|---|---|
| $SiO_2$ | 67.14 | 64.65 | 65.96 | 63.59 | 77.22 | 63.44 | 71.1 | 67.16 | 64.43 | 65.98 |
| $TiO_2$ | 0.43 | 0.84 | 0.44 | 0.63 | 0.09 | 0.53 | 0.19 | 0.41 | 0.49 | 0.51 |
| $Al_2O_3$ | 16.25 | 16.77 | 17 | 16.77 | 12.71 | 17.3 | 16.13 | 16.57 | 17.52 | 16.33 |
| $Fe_2O_3$ | 3.1 | 4.88 | 3.18 | 3.39 | 0.49 | 3.6 | 1.59 | 2.77 | 3.53 | 4.03 |
| MnO | 0.06 | 0.06 | 0.06 | 0.06 | 0.01 | 0.07 | 0.04 | 0.05 | 0.06 | 0.04 |
| MgO | 1.85 | 2.78 | 1.91 | 2.77 | 0.06 | 2.56 | 0.77 | 1.78 | 1.83 | 1.87 |
| CaO | 4.24 | 0.88 | 4.37 | 5.05 | 0.55 | 2.15 | 2.8 | 4.06 | 4.18 | 2.12 |
| $Na_2O$ | 4.87 | 2.26 | 4.82 | 4.98 | 3.62 | 4.96 | 5.1 | 4.96 | 4.6 | 2.86 |
| $K_2O$ | 1.42 | 4.95 | 1.62 | 1.61 | 4.88 | 1.76 | 1.49 | 1.43 | 1.42 | 1.8 |
| $P_2O_5$ | 0.17 | 0.14 | 0.16 | 0.21 | 0.02 | 0.23 | 0.11 | 0.15 | 0.18 | 0.02 |
| LOI | 0.4 | 1.6 | 0.4 | 0.7 | 0.4 | 3.3 | 0.6 | 0.6 | 1.7 | 4.4 |
| TOTAL | 99.93 | 99.81 | 99.92 | 99.76 | 100.05 | 99.90 | 99.92 | 99.94 | 99.94 | 99.96 |
| Ni | 9.2 | 38 | 11.1 | 9.7 | 0.5 | 31.6 | 4.1 | 11.9 | 9.6 | 15.1 |
| Sc | 7 | 13 | 7 | 9 | 1 | 9 | 3 | 6 | 8 | 8 |
| Ba | 398 | 1578 | 362 | 345 | 121 | 265 | 571 | 367 | 322 | 404 |
| Be | 1 | 2 | 1 | 2 | 2 | 1 | 1 | 1 | 2 | 2 |
| Co | 9.3 | 11.5 | 10.6 | 12.6 | 0.9 | 11.1 | 3.2 | 8.7 | 10.3 | 12.7 |
| Cs | 0.7 | 5.8 | 0.6 | 1.1 | 0.5 | 1.2 | 1.3 | 1 | 1 | 8.4 |
| Ga | 17.3 | 25 | 18.1 | 17.8 | 14.9 | 18.9 | 17.5 | 17.5 | 18.1 | 21.2 |
| Hf | 2 | 5.8 | 3.7 | 3.3 | 3.6 | 3 | 2.3 | 3.5 | 3.3 | 3.2 |
| Nb | 12.6 | 12.9 | 11.7 | 16.5 | 19.5 | 18.8 | 7.3 | 9.1 | 11.4 | 13.3 |
| Rb | 29 | 182 | 35 | 39 | 66 | 59 | 32 | 39 | 36 | 84 |
| Sr | 673 | 92 | 692 | 757 | 42 | 769 | 683 | 675 | 650 | 392 |
| Ta | 1 | 1 | 1 | 1.1 | 3.1 | 1.4 | 0.6 | 0.6 | 0.9 | 1.1 |
| Th | 4 | 8 | 4 | 5 | 25 | 6 | 4 | 3 | 5 | 8 |
| U | 1 | 2.4 | 1.3 | 1.9 | 6.2 | 1.8 | 1.2 | 1.3 | 1.7 | 1.3 |
| V | 73 | 109 | 72 | 86 | 10 | 76 | 22 | 60 | 72 | 94 |
| W | 0.1 | 5 | 0.1 | 0.5 | 0.8 | 0.5 | 0.1 | 0.1 | 0.1 | 0.3 |
| Zr | 64 | 190 | 118 | 112 | 68 | 116 | 73 | 122 | 107 | 107 |
| Y | 11 | 33 | 10 | 11 | 8 | 10 | 9 | 7 | 10 | 7 |
| La | 17.9 | 32.3 | 16.6 | 18.6 | 19.1 | 22.5 | 16.8 | 14.1 | 17.9 | 22.7 |
| Ce | 36.7 | 66.9 | 31.6 | 36.5 | 35.8 | 40.3 | 31.6 | 26.5 | 34.6 | 33.3 |
| Pr | 4.18 | 8.49 | 3.56 | 4.28 | 3.69 | 4.52 | 3.55 | 3.07 | 3.93 | 3.75 |
| Nd | 14.9 | 32.7 | 13.2 | 16.7 | 12.4 | 16.8 | 12.3 | 11.4 | 14.3 | 13.6 |
| Sm | 2.72 | 6.4 | 2.38 | 2.93 | 1.91 | 2.83 | 2.28 | 2.01 | 2.66 | 1.97 |
| Eu | 0.7 | 1.22 | 0.68 | 0.84 | 0.26 | 0.85 | 0.64 | 0.65 | 0.77 | 0.62 |
| Gd | 2.25 | 5.42 | 1.97 | 2.31 | 1.38 | 2.09 | 1.69 | 1.55 | 1.98 | 1.48 |
| Tb | 0.36 | 0.99 | 0.33 | 0.38 | 0.26 | 0.36 | 0.28 | 0.25 | 0.33 | 0.21 |
| Dy | 1.82 | 5.47 | 1.63 | 1.87 | 1.35 | 1.81 | 1.39 | 1.4 | 1.67 | 0.98 |
| Ho | 0.34 | 1.1 | 0.3 | 0.33 | 0.24 | 0.33 | 0.27 | 0.22 | 0.31 | 0.19 |
| Er | 0.93 | 3.02 | 0.87 | 0.97 | 0.84 | 0.96 | 0.79 | 0.65 | 0.98 | 0.54 |
| Tm | 0.16 | 0.49 | 0.14 | 0.15 | 0.13 | 0.14 | 0.1 | 0.09 | 0.14 | 0.1 |
| Yb | 0.94 | 2.87 | 0.82 | 0.84 | 1.02 | 0.83 | 0.7 | 0.66 | 0.92 | 0.6 |
| Lu | 0.14 | 0.45 | 0.14 | 0.13 | 0.17 | 0.14 | 0.1 | 0.1 | 0.14 | 0.1 |
| Eu/Eu* | 0.87 | 0.63 | 0.96 | 0.99 | 0.49 | 1.07 | 1.00 | 1.13 | 1.03 | 1.11 |
| (La/Lu)N | 13.27 | 7.45 | 12.31 | 14.85 | 11.66 | 16.68 | 17.44 | 14.64 | 13.27 | 23.56 |
| ASI | 0.94 | 1.59 | 0.97 | 0.88 | 1.05 | 1.24 | 1.07 | 0.97 | 1.05 | 1.56 |
| Mg# | 51.55 | 50.38 | 51.71 | 59.29 | 17.92 | 55.90 | 46.33 | 53.39 | 48.03 | 45.27 |
| (Yb)N | 1.91 | 5.82 | 1.66 | 1.70 | 2.07 | 1.68 | 1.42 | 1.34 | 1.87 | 1.22 |
| (La/Yb)N | 13.17 | 7.78 | 14.00 | 15.31 | 12.95 | 18.74 | 16.59 | 14.77 | 13.45 | 26.16 |

**Explanations:** Mg#= 100x(Mol MgO/MgO+$FeO^{tot}$); Eu/Eu*= $(Eu/Eu_N)/[\sqrt{(Sm/Sm_N)x(Gd/Gd_N)}]$

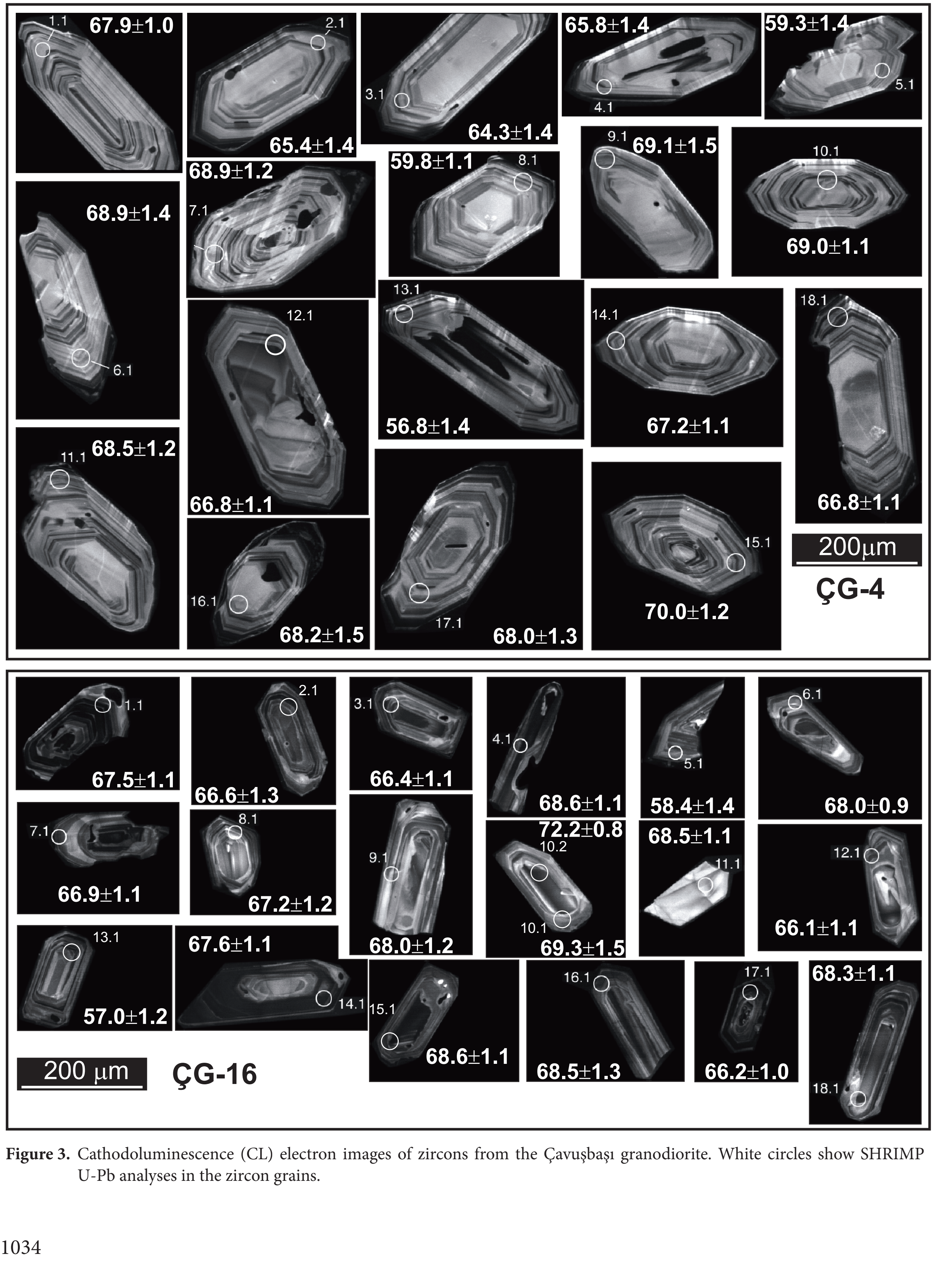


**Figure 3.** Cathodoluminescence (CL) electron images of zircons from the Çavuşbaşı granodiorite. White circles show SHRIMP U-Pb analyses in the zircon grains.

The U-Th-Pb analyses were made using SHRIMP-II at the Research School of Earth Sciences, The Australian National University, Canberra, Australia following procedures given in Williams (1998). Each analysis consisted of 6 scans through the mass range, with the Temora reference zircon grains analyzed for every three unknown analyses. The data have been reduced using the SQUID Excel Macro of Ludwig (2001). The Pb/U ratios have been normalised relative to a value of 0.0668 for the Temora reference zircon, equivalent to an age of 417 Ma (see Black *et al.* 2003). Uncertainties given for individual analyses (ratios and ages) are at the one sigma level (Table 2). Tera & Wasserburg (1972) concordia plots, probability density plots with stacked histograms and weighted mean $^{206}Pb/^{238}U$ age calculations were carried out using ISOPLOT/EX (Ludwig 2003). Weighted mean $^{206}Pb/^{238}U$ ages were calculated and the uncertainties are reported at 95% confidence limits.

The potassium content was determined using a spectrophotometer Sherwood 420. During the measurements international standard 'Cordoba muscovite' was used to test the procedure. The analytical error was 0.02% $K_2O$. The isotopic composition of Ar was determined by the extraction method (details in Bonhomme *et al.* 1975) using an MS20 mass spectrometer Lewandowska *et al.* (2007). Analytical precision was periodically controlled by the measurements of the radiogenic $^{40}Ar$ content of the international standard GLO. The overall precision of the K-Ar age determinations, which were calculated using the decay constant recommended by Steiger & Jaeger (1977), was better than ±2 %. K-Ar age determinations were performed at the Institute of Geological Sciences, Polish Academy of Sciences (Table 3).

Sr and Nd isotope analyses were performed at the radiogenic isotope laboratory of METU Central Laboratory (Ankara) with standard cation exchange methods as described by Köksal & Göncüoğlu (2008). During the analyses BCR-1 USGS standard was processed in the same conditions, and $^{87}Sr/^{86}Sr$= 0.705014±5 and $^{143}Nd/^{144}Nd$= 0.512638±4 ratios were obtained. Analytical uncertainties are given at $2\sigma_m$ level. No corrections were applied to Nd and Sr isotopic compositions for instrumental bias (Table 4).

**Petrography**

The Çavuşbaşı intrusion comprises medium-grained granodiorite, tonalite and subordinate quartz diorite. The pluton contains quartz, plagioclase, K-feldspar (orthoclase), hornblende, biotite, and accessory titanite, apatite, zircon and opaque minerals. Plagioclase ($An_{32-38}$) occurs as euhedral to subhedral grains and often shows polysynthtetic zoning. Sericitization of plagioclase is common. K-feldspar shows generally perthite structure and plagioclase and orthoclase are often found in other minerals (quartz, hornblende, biotite, opaque, etc.) as inclusions. Hornblende is subhedral and is associated with biotite, epidote, titanite and opaques. The coarse-grained hornblende often shows transition to biotite along its cleavages and is sometimes granulated along its edges, and enclosed by plagioclase. The biotite in the granodiorite is greenish brown, euhedral-subhedral, with a prismatic-flaky habit. Hornblende and biotite are rarely altered to chlorite and secondary epidote. Both the Çavuşbaşı granodiorite and its mafic microgranular enclaves (MMEs) include some special mixing textures such as antirapakivi, blade-shaped biotite, acicular apatite, spongy cellular plagioclase (Figure 2c), poikilitic feldspar (Figure 2d), and dissolution/melting plagioclase textures (Hibbard 1991). MMEs are holocrystalline, fine-grained, occasionally with a porphyritic texture and have similar mineral assemblage to their host rocks. Aplitic vein rocks have a felsic mineralogy, with plagioclase, quartz, K-feldspars and microcline. Rarely, they include biotite and sericite/muscovite. The microdiorites are composed of plagioclase, hornblende and biotite.

**Geochronology**

Table 2 shows the analytical data for U-Pb zircon dating via SHRIMP-II on thirty-six grains from two samples (ÇG-4 and ÇG-16). Zircon grains from the Çavuşbaşı granodiorite are 100–200 µm long and prismatic, are euhedral to subhedral with oscillatory zoning typical of magmatic growth (Figure 3). Some zircon grains are broken and have corroded outlines. The zircon grains are concordant, yielding weighted means of 67.91±0.63 Ma (2s, MSWD= 0.57) and 67.59±0.5 Ma (2s, MSWD= 0.94) (Figure 4). Based on the the high concordance of zircon grains and

**Table 2**. SHRIMP U-Pb radiometric age data from the Çavuşbaşı granodiorite.

| **ÇG–4** | | | | | | | Total | | | | Radiogenic Age (Ma) | | | |
|---|---|---|---|---|---|---|---|---|---|---|---|---|---|---|
| Grain spot | U (ppm) | Th (ppm) | Th/U | $^{206}Pb^*$ (ppm) | $^{204}Pb/^{206}Pb$ | $f_{206}$ % | $^{238}U/^{206}Pb$ | ± | $^{207}Pb/^{206}Pb$ | ± | $^{206}Pb/^{238}U$ | ± | $^{206}Pb/^{238}U$ | ± |
| 1.1 | 313 | 254 | 0.81 | 2.9 | 0.001502 | 0.57 | 93.93 | 1.38 | 0.0519 | 0.0017 | 0.0106 | 0.0002 | 67.9 | 1.0 |
| 2.1 | 107 | 48 | 0.45 | 1.0 | 0.004101 | 2.17 | 95.90 | 2.05 | 0.0645 | 0.0041 | 0.0102 | 0.0002 | 65.4 | 1.4 |
| 3.1 | 152 | 65 | 0.43 | 1.3 | 0.000196 | 0.79 | 98.94 | 2.05 | 0.0535 | 0.0030 | 0.0100 | 0.0002 | 64.3 | 1.4 |
| 4.1 | 130 | 60 | 0.46 | 1.2 | – | 2.50 | 95.05 | 1.97 | 0.0671 | 0.0035 | 0.0103 | 0.0002 | 65.8 | 1.4 |
| 5.1 | 144 | 62 | 0.43 | 1.2 | 0.003110 | 0.92 | 107.29 | 2.54 | 0.0545 | 0.0036 | 0.0092 | 0.0002 | 59.3 | 1.4 |
| 6.1 | 120 | 47 | 0.39 | 1.1 | 0.003410 | 1.35 | 91.86 | 1.82 | 0.0581 | 0.0028 | 0.0107 | 0.0002 | 68.9 | 1.4 |
| 7.1 | 185 | 127 | 0.69 | 1.7 | 0.001083 | 0.45 | 92.59 | 1.54 | 0.0509 | 0.0020 | 0.0108 | 0.0002 | 68.9 | 1.2 |
| 8.1 | 256 | 174 | 0.68 | 2.1 | – | 0.22 | 107.13 | 2.00 | 0.0489 | 0.0025 | 0.0093 | 0.0002 | 59.8 | 1.1 |
| 9.1 | 203 | 78 | 0.39 | 1.9 | 0.000683 | <0.01 | 93.16 | 2.06 | 0.0442 | 0.0028 | 0.0108 | 0.0002 | 69.1 | 1.5 |
| 10.1 | 203 | 113 | 0.55 | 1.9 | 0.000488 | 0.95 | 92.10 | 1.49 | 0.0549 | 0.0020 | 0.0108 | 0.0002 | 69.0 | 1.1 |
| 11.1 | 189 | 83 | 0.44 | 1.8 | 0.001135 | 1.19 | 92.55 | 1.55 | 0.0568 | 0.0022 | 0.0107 | 0.0002 | 68.5 | 1.2 |
| 12.1 | 292 | 161 | 0.55 | 2.6 | 0.000673 | 0.53 | 95.43 | 1.50 | 0.0516 | 0.0019 | 0.0104 | 0.0002 | 66.8 | 1.1 |
| 13.1 | 311 | 170 | 0.54 | 2.4 | 0.002724 | 0.53 | 112.33 | 2.81 | 0.0513 | 0.0038 | 0.0089 | 0.0002 | 56.8 | 1.4 |
| 14.1 | 186 | 102 | 0.55 | 1.7 | 0.001647 | 0.52 | 94.92 | 1.57 | 0.0515 | 0.0020 | 0.0105 | 0.0002 | 67.2 | 1.1 |
| 15.1 | 191 | 93 | 0.49 | 1.8 | – | 0.68 | 90.95 | 1.49 | 0.0528 | 0.0020 | 0.0109 | 0.0002 | 70.0 | 1.2 |
| 16.1 | 91 | 36 | 0.40 | 0.8 | 0.000716 | 1.23 | 92.85 | 2.06 | 0.0571 | 0.0033 | 0.0106 | 0.0002 | 68.2 | 1.5 |
| 17.1 | 131 | 67 | 0.51 | 1.2 | 0.001201 | 1.75 | 92.64 | 1.78 | 0.0612 | 0.0036 | 0.0106 | 0.0002 | 68.0 | 1.3 |
| 18.1 | 344 | 191 | 0.55 | 3.1 | 0.000196 | 0.56 | 95.12 | 1.33 | 0.0518 | 0.0015 | 0.0105 | 0.0001 | 67.0 | 0.9 |

| **ÇG–16** | | | | | | | Total | | | | Radiogenic Age (Ma) | | | |
|---|---|---|---|---|---|---|---|---|---|---|---|---|---|---|
| Grain spot | U (ppm) | Th (ppm) | Th/U | $^{206}Pb^*$ (ppm) | $^{204}Pb/^{206}Pb$ | $f_{206}$ % | $^{238}U/^{206}Pb$ | ± | $^{207}Pb/^{206}Pb$ | ± | $^{206}Pb/^{238}U$ | ± | $^{206}Pb/^{238}U$ | ± |
| 1.1 | 221 | 93 | 0.42 | 2.0 | – | 0.81 | 94.18 | 1.52 | 0.0538 | 0.0020 | 0.0105 | 0.0002 | 67.5 | 1.1 |
| 2.1 | 182 | 78 | 0.43 | 1.7 | 0.000754 | 3.80 | 92.68 | 1.59 | 0.0775 | 0.0080 | 0.0104 | 0.0002 | 66.6 | 1.3 |
| 3.1 | 203 | 100 | 0.49 | 1.8 | 0.001191 | 0.86 | 95.70 | 1.55 | 0.0541 | 0.0029 | 0.0104 | 0.0002 | 66.4 | 1.1 |
| 4.1 | 226 | 101 | 0.45 | 2.1 | 0.001201 | 1.17 | 92.40 | 1.43 | 0.0567 | 0.0019 | 0.0107 | 0.0002 | 68.6 | 1.1 |
| 5.1 | 248 | 149 | 0.60 | 1.9 | – | 0.09 | 109.73 | 2.54 | 0.0479 | 0.0032 | 0.0091 | 0.0002 | 58.4 | 1.4 |
| 6.1 | 512 | 327 | 0.64 | 4.7 | 0.000151 | 0.93 | 93.39 | 1.23 | 0.0548 | 0.0014 | 0.0106 | 0.0001 | 68.0 | 0.9 |
| 7.1 | 195 | 85 | 0.44 | 1.8 | – | 0.83 | 95.10 | 1.55 | 0.0540 | 0.0021 | 0.0104 | 0.0002 | 66.9 | 1.1 |
| 8.1 | 187 | 75 | 0.40 | 1.7 | 0.001327 | 1.90 | 93.56 | 1.58 | 0.0624 | 0.0023 | 0.0105 | 0.0002 | 67.2 | 1.2 |
| 9.1 | 158 | 76 | 0.48 | 1.5 | 0.000931 | 2.16 | 92.23 | 1.67 | 0.0645 | 0.0026 | 0.0106 | 0.0002 | 68.0 | 1.2 |
| 10.1 | 93 | 36 | 0.39 | 0.9 | 0.000470 | 2.81 | 89.97 | 1.92 | 0.0697 | 0.0036 | 0.0108 | 0.0002 | 69.3 | 1.5 |
| 10.2 | 1131 | 750 | 0.66 | 11.0 | 0.000068 | 0.25 | 88.57 | 1.03 | 0.0494 | 0.0008 | 0.0113 | 0.0001 | 72.2 | 0.8 |
| 11.1 | 186 | 77 | 0.42 | 1.7 | 0.001313 | 1.23 | 92.42 | 1.53 | 0.0571 | 0.0021 | 0.0107 | 0.0002 | 68.5 | 1.1 |
| 12.1 | 189 | 87 | 0.46 | 1.7 | – | 1.04 | 96.01 | 1.61 | 0.0556 | 0.0022 | 0.0103 | 0.0002 | 66.1 | 1.1 |
| 13.1 | 204 | 94 | 0.46 | 1.6 | 0.001007 | 0.99 | 111.57 | 2.24 | 0.0550 | 0.0029 | 0.0089 | 0.0002 | 57.0 | 1.2 |
| 14.1 | 194 | 77 | 0.39 | 1.8 | 0.001839 | 1.38 | 93.56 | 1.51 | 0.0583 | 0.0021 | 0.0105 | 0.0002 | 67.6 | 1.1 |
| 15.1 | 232 | 110 | 0.47 | 2.1 | – | 0.55 | 92.95 | 1.42 | 0.0518 | 0.0018 | 0.0107 | 0.0002 | 68.6 | 1.1 |
| 16.1 | 152 | 74 | 0.49 | 1.4 | 0.000825 | 0.89 | 92.82 | 1.74 | 0.0545 | 0.0023 | 0.0107 | 0.0002 | 68.5 | 1.3 |
| 17.1 | 263 | 141 | 0.54 | 2.4 | 0.000502 | 0.80 | 96.07 | 1.41 | 0.0536 | 0.0018 | 0.0103 | 0.0002 | 66.2 | 1.0 |
| 18.1 | 182 | 91 | 0.50 | 1.7 | 0.000178 | 0.66 | 93.33 | 1.54 | 0.0526 | 0.0021 | 0.0106 | 0.0002 | 68.3 | 1.1 |

**Table 3.** K-Ar radiometric data from amphibol in the Çavuşbaşı granodiorite.

| Name | Mineral | Fraction (mm) | Weight [mg] | % K | % $K_2O$ | % $^{40}Ar^*$ | $^{40}Ar^*$ [pmol/g] | Age [My] | Error [My] |
|---|---|---|---|---|---|---|---|---|---|
| CG-16 | Amphibole | 0.18–0.35(mm) | 81.54 | 1.19 | 1.43 | 7.9 | 133.0 | 63.5 | ±1.6 |

**Table 4.** Sr and Nd isotopic data from the Çavuşbaşı granodiorite.

| Sample | Age (Ma) | Sr | Rb | Sm | Nd | $^{87}Rb/^{86}Sr$ | $^{87/86}Sr$ | $^{87/86}Sr$ (i) | $^{147}Sm/^{144}Nd$ | $^{143/144}Nd$ | $^{143/144}Nd(i)$ | εNd(t) |
|---|---|---|---|---|---|---|---|---|---|---|---|---|
| **ÇG-4** | 68 | 692 | 35 | 2.38 | 13.2 | 0.1442 | 0.703694 | **0.703555** | 0.1095 | 0.512765 | **0.512716** | **3.2** |
| **ÇG-16** | 68 | 675 | 39 | 2.01 | 11.4 | 0.1671 | 0.703669 | **0.703509** | 0.1071 | 0.512788 | **0.512741** | **3.7** |

the typical magmatic growth, these age values are regarded as the crystallization age of the Çavuşbaşı granodiorite.

K-Ar age of the separated hornblende and biotite from the Çavuşbaşı adakitic granodiorite is 63.5±1.6 Ma in only one sample (ÇG-16). This age value is in close agreement with the Rb-Sr whole rock age value of 63±13 Ma reported by Öztunalı & Satır (1975).

## Geochemistry

Major and trace element concentrations for the Çavuşbaşı granodiorite are given in Table 1. Çavuşbaşı granodiorite samples plot in the granodiorite, tonalite and quartz monzodiorite fields in the Q[100Q/(Q+Or+Ab+An)] versus ANOR [100An/(An+Or)] diagram (Figure 5; Streckeisen & Le Maitre 1979). The Çavuşbaşı granodiorite plots in the middle-K calc-alkaline series area on a $SiO_2$–$K_2O$ diagram, (Figure 6a; Pecerillo & Taylor 1976). The aluminium saturation values range from 0.9 to 1.6, suggesting a metaluminous to perlauminous affinity. The aplitic samples (ÇG-2, ÇG-7) have relatively higher ASI values (1.1–1.6) due to presence of sericite and clay minerals (Figure 6b).

The Upper Cretaceous Çavuşbaşı granodiorite has $SiO_2$ exceeding 63.59 wt%, and high $Al_2O_3$ (>16.13 wt%) contents (Table 1). The $Al_2O_3$, $Fe_2O_3$, MgO, $TiO_2$ and $P_2O_5$ contents decrease with increasing $SiO_2$ on Harker digrams (Figure 7). No distinctive pattern is seen in the CaO, $K_2O$ and $Na_2O$ values. $K_2O$ values are between 1–2 wt%, but $Na_2O$ values generally exceed 2 wt% (Figure 7). MgO contents of Çavuşbaşı granodiorite samples are usually less than 3 wt% (0.77–2.77 wt%) and are associated with a narrow range of Mg# (45.27–59.29) (Table 1). There is a weak negative correlation between Rb, Sc, Co and $SiO_2$, but the Sr content shows rising trends with increasing $SiO_2$ contents in Figure 7.

On the multi-element variation diagrams normalized to the primitive mantle (PRIM; Sun & McDonough 1989) the Çavuşbaşı pluton shows negative anomalies of Nb,Ta, Pb, P and Ti, but positive anomalies of U, K and Sr (Figure 8a). Chondrite-normalized rare earth element (REE) patterns are characterized by highly fractionated LREE relative to HREE ($La_N/Yb_N$–13-26) and the general absence of a pronounced negative Eu anomaly (Eu/Eu* 0.87–1.13) (Figure 8b). The Upper Cretaceous Çavuşbaşı granodiorite displays characteristics of adakitic rocks with high Sr/Y (>59.33) and low Y (6.60–10.7 ppm) and Yb (0.60–1.02 ppm) (Table 2). All the samples plot in the adakitic field on the Sr/Y–Y and $(La/Yb)_N$–$(Yb)_N$ diagrams (Figure 9a, b). In addition, the Çavuşbaşı pluton is characterized by high contents of Sr, LREE, and low contents of Y, HREE, resulting in high ratios of Sr/Y and $(La/Yb)_N$ . With these characteristics the Çavuşbaşı intrusion resembles adakites (Figure 9a, b; Defant & Drummond 1990; Castillo *et al.* 1999; Condie 2005). $^{87/86}Sr_{(i)}$ and

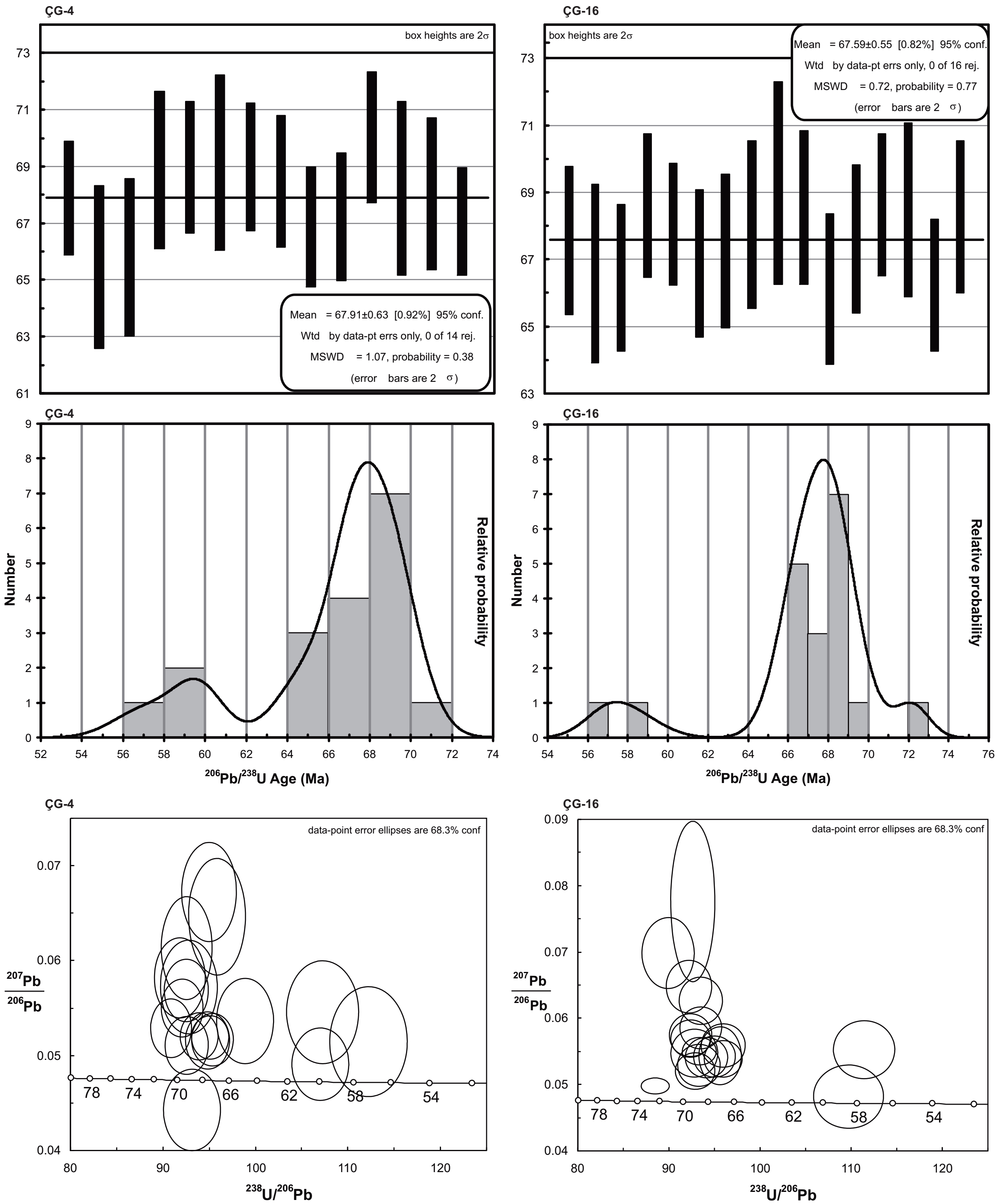


**Figure 4.** U-Pb SHRIMP zircon data from the Çavuşbaşı granodiorite **(a)** sample ÇG-4 **(b)** sample ÇG-16. The Pb/U ratios have been normalized relative to a value of 0.0668 for the Temora reference zircon, equivalent to an age of 417 Ma (Black *et al.* 2003).

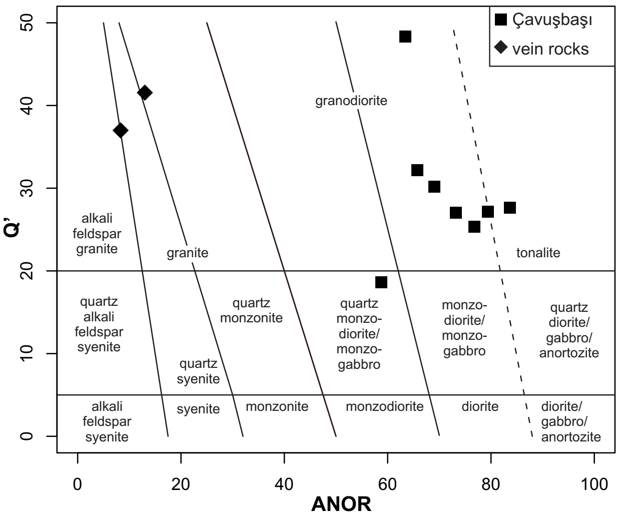


**Figure 5.** Q[100Q/(Q+Or+Ab+An)] versus ANOR [100An/(An+Or)] nomenclature diagram (Streckeisen & Le Maitre 1979) for the Çavuşbaşı granodiorite.

$^{143}$/$^{144}$Nd$_{(i)}$ values of two samples (ÇG-4, ÇG-16) from Çavuşbaşı granodiorite are 0.7035–0.7036 and 0.512716–0.512740, respectively (Table 3).

## Discussion

The Strandja, İstanbul and Sakarya zones as a whole are defined as the Pontides. The Pontides are separated by the İzmir-Ankara-Erzincan suture from the Anatolide-Tauride block (Okay & Tüysüz 1999). Also, the Intra-Pontide suture between the İstanbul and Sakarya zones formed a plate boundary during the Cretaceous. The oceanic domains between these continental domains were consumed by northward subduction (Şengör & Yılmaz 1981; Okay & Şahintürk 1997; S. Yılmaz & Boztuğ 1996; Okay *et al.* 1996; Boztuğ *et al.* 2006). Upper Cretaceous andesitic lavas, dykes and small acidic intrusions, which are widespread in the western part of İstanbul Zone, were considered as products of the arc magmatism related to the northward subduction of either the Intra-Pontide or İzmir-Ankara-Erzincan oceans (Şengör & Yılmaz 1981; Y. Yılmaz *et al.* 1995; Okay & Şahintürk 1997; Okay & Tüysüz 1999; Robertson & Ustaömer 2004; Altherr *et al.* 2008; Topuz *et al.* 2008). Hence the adakitic Çavuşbaşı granodiorite (~68 Ma) was formed in an active subductional setting, rather than a post-collisional one. This is a major difference from

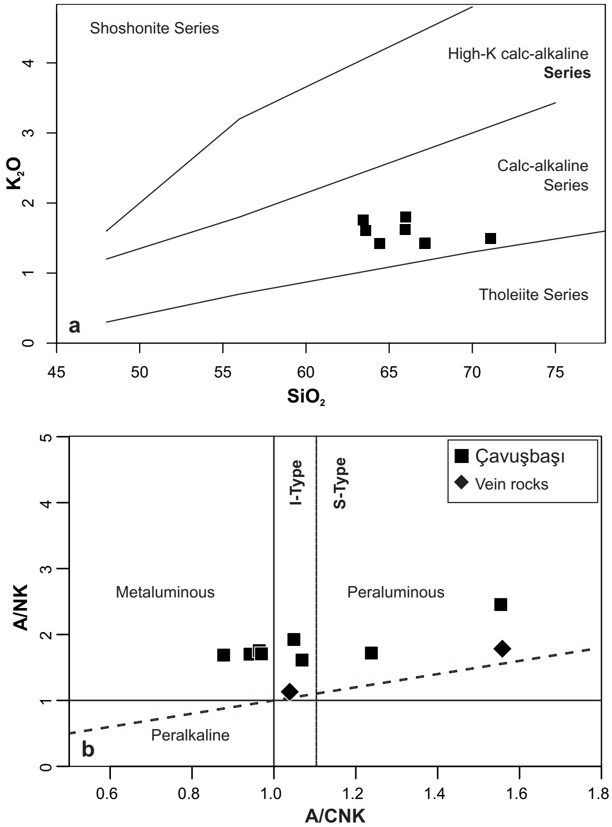


**Figure 6.** Plots of the Çavuşbaşı granodiorite samples: **(a)** $K_2O$–$SiO_2$ diagram (Pecerillo & Taylor 1976), **(b)** A/NK–A/CNK diagram (Maniar & Piccoli 1989).

the adakitic plutonic and volcanic rocks in the Eastern Pontides, which were formed in the Palaeocene to Early Eocene (48–55 Ma) in a post-collisional setting (Topuz *et al.* 2005, 2011; Karslı *et al.* 2007; Kadıoğlu & Dilek 2010; Eyüboğlu *et al.* 2011).

The known Late Cretaceous intrusions and volcanics in the Western Pontides differ geochemically from the Çavuşbaşı granodiorite (e.g., Keskin *et al.* 2003, 2010; Karacık & Tüysüz 2010). For example, the Demirköy pluton is characterized by slightly fractionated rare earth element patterns with a pronounced Eu anomaly, ruling out the presence of garnet as a residual mineral. They also display more enriched Sr-Nd isotopic signatures in clear distinction to the Çavuşbaşı granodiorite (Figure 10a).

Adakitic melts can be generated by (i) direct melting of the downgoing subducted oceanic slab at convergent margins (Defant & Drummond 1990; Kay

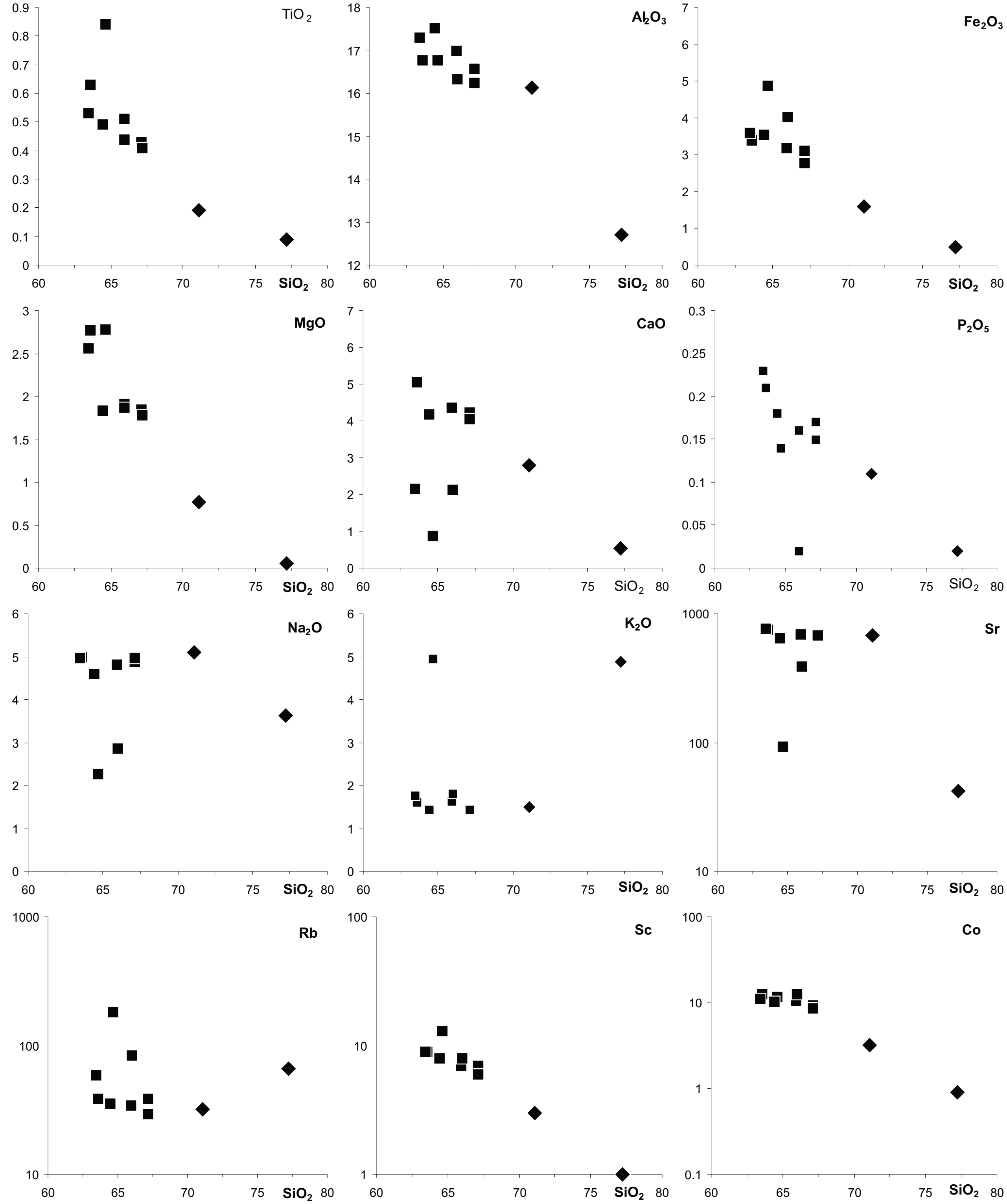


**Figure 7.** Harker variation diagrams for selected major (wt%) and trace (ppm) elements of the Çavuşbaşı granodiorite.

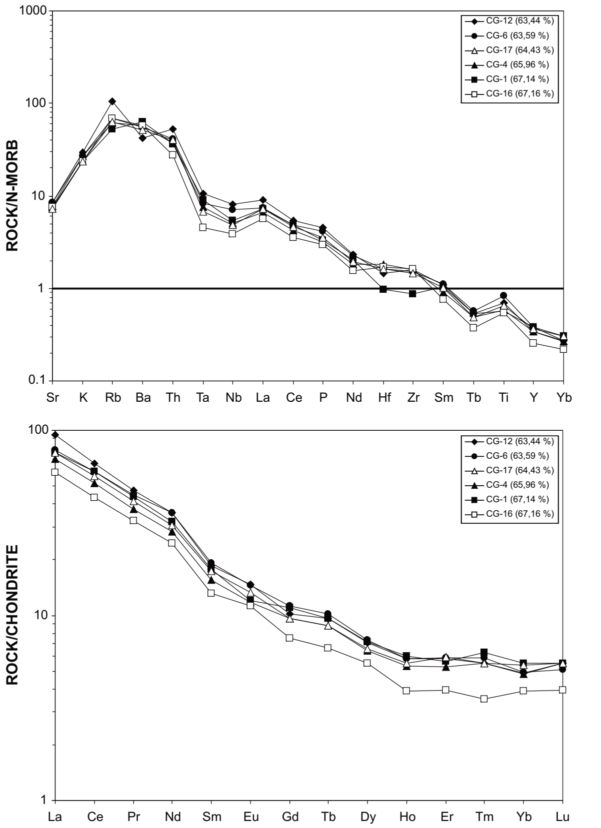


**Figure 8.** **(a)** PRIM-normalized diagram (Sun & McDonough 1989) for trace elements of the Çavuşbaşı metagranite, **(b)** CHONDRITE-normalized diagram (Sun & McDonough 1989) for REE of the Çavuşbaşı granodiorite.

*et al.* 1993; Stern & Kilian 1996), (ii) partial melting of thickened mafic lower crust (Atherton & Petford 1993; Hou *et al.* 2004; Topuz *et al.* 2005, 2011; Karslı *et al.* 2010) and (iii) high-pressure fractionation of mantle-wedge derived magmas (Castillo *et al.* 1999; Macpherson *et al.* 2006). The MgO (0.77–2.56 wt%) and Mg# (45.27–59.29) contents of the Çavuşbaşı granodiorite are relatively high, requiring interaction with mantle peridotite (Figure 10b). However, the Cavuşbaşı granodiorite is similar to the partial melts of metabasic rocks in terms of $(Na_2O+K_2O)/(FeO+MgO+TiO_2)$ vs $Na_2O+K_2O+FeO+MgO+TiO_2)$ (Patiňo Douce 1999; Figure 10c). On the basis of depleted Sr-Nd isotopy, and formation in an active subduction setting, we suggest that the melt of the Çavuşbaşı granodiorite was a product of partial melting of a Neo-Tethyan oceanic slab and later interaction with the mantle-peridotite.

## Conclusions

1. The Çavuşbaşı granodiorite is located in the İstanbul Zone of the western Pontides, and has a fine- to medium-grained granodioritic and tonalitic composition, with a generally metaluminous, middle-K, calk-alkaline I-type character.

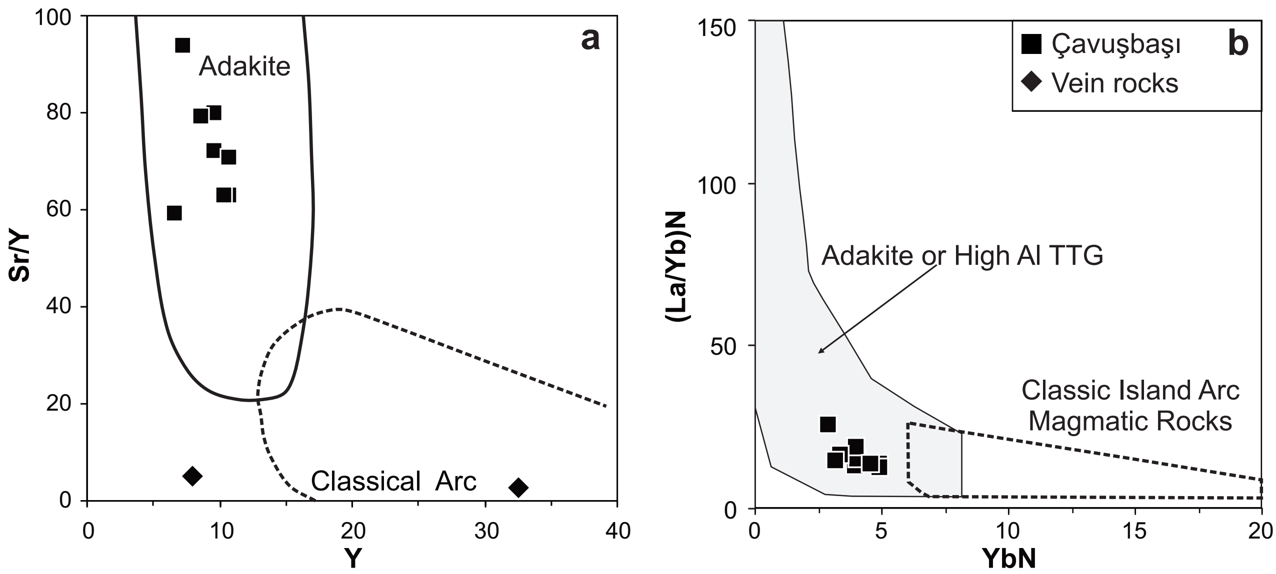


**Figure 9.** **(a)** Sr/Y–Y, **b)** La/Yb–Yb diagrams (Defant & Drummond 1990) for the adakitic Çavuşbaşı granodiorite.

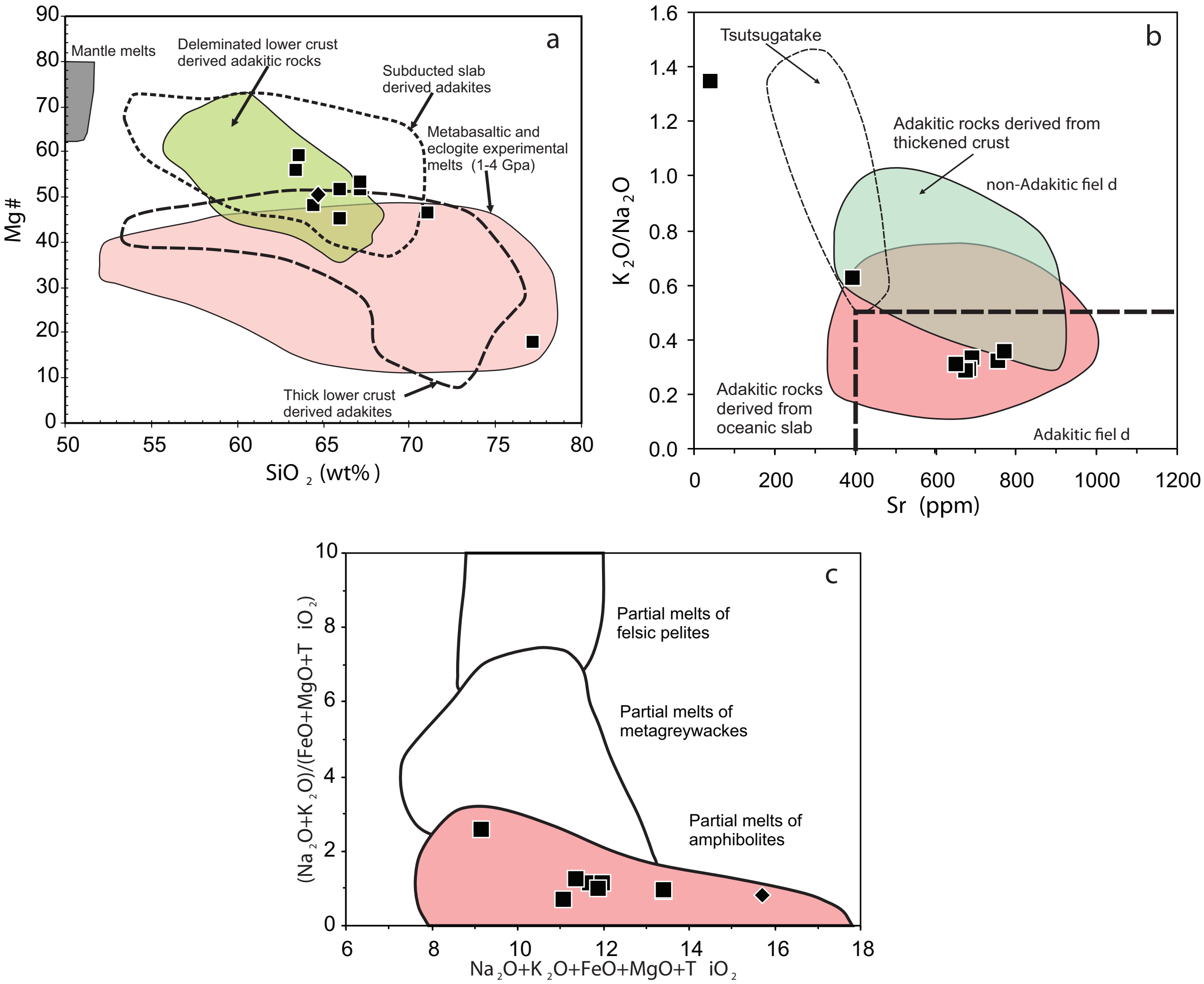


**Figure 10.** **(a)** $^{43}$Nd/$^{144}$Nd - $^{87}$Sr/$^{86}$Sr diagrams for adakitic Çavuşbaşı granodiorite (Patiňo Douce 1999). MORB, EMI and EMII fields are from Hoffmann (1997) and DMM (Depleted MORB mantle) is from Workman & Hart (2005). The data of Phillippine Sea Plate rocks and the other Cenozoic rocks taken from Macpherson *et al.* 2006. **(b)** Mg#–$SiO_2$ diagram for the Çavuşbaşı granodiorite; **(c)** ($Na_2O+K_2O$)/($FeO+MgO+TiO_2$) – $Na_2O+K_2O+FeO+MgO+TiO_2$ diagram for the Çavuşbaşı granodiorite (partial melting of felsic pelites, metagreywackes, and amphibolites obtained in experimental studies (Patiňo Douce 1999).

**2.** In-situ zircon dating on two samples indicates emplacement during the Late Cretaceous (67.91±0.63 Ma and 67.59±0.5 Ma). The K/Ar hornblende age is also 64 Ma.

**3.** The Çavuşbaşı granodiorite resembles high-silica adakites from supra-subduction zone settings with high Sr/Y, La/Yb, Mg# (45.27–55.90), MgO (0.77–2.56 wt%) and low Y (6.60–10.7 ppm), Yb (0.60–1.02 ppm), and HREE values.

**4.** The granodiorite is characterized by relatively low, depleted Sr-Nd isotopy ($^{87/86}Sr_{(i)}$= 0.703508–0.703555 and high $^{143/144}Nd_{(i)}$= 0.512716–0.512740, εNd($t$) = 3.2–3.7 values).

**5.** The Çavuşbaşı granodiorite was most probably generated from the partial melting of a subducted oceanic slab of the northern branch of Neo-Tethyan Ocean.

## Acknowledgements

This study was financed by the İstanbul University Research Foundation (Project Numbers:

435/13092005 and 436/13092005). We thank G. Sunal, N. Okay and A.I. Okay and for their help in the mineral seperation laboratories of the İstanbul Technical University. We also thank A. Yurdagül-Ceyhan for her help during the fieldwork. We thank Gültekin Topuz and an anonymous referee for helpful comments that have significantly improved an earlier version of the manuscript.

## References

Abdüsselâmoğlu, Ş. 1963. *Kocaeli Yarımadası'nın Jeolojisi [Geology of Kocaeli Peninsula]*. Mineral Research and Exploration Institute of Turkey (MTA) Report no. **3249** [in Turkish, unpublished].

Altherr, R., Topuz, G., Siebel, W., Şen, C., Meyer, H.-P. & Satir, M. 2008. Geochemical and Sr-Nd-Pb isotopic characteristics of Paleocene plagioleucitites from the Eastern Pontides (NE Turkey). *Lithos* **105**, 149–161.

Atherton, M.P. & Petford, N. 1993. Generation of sodium-rich magmas from newly underplated basaltic crust. *Nature* **362**, 144–146.

Barbarin, B. & Didier, J. 1992. Genesis and evolution of mafic microgarnular enclaves through various types of interaction between coexting felsic and mafic magmas. *Transactions of the Royal Society of Edinburgh, Earth Sciences* **83**, 145–153.

Black, L.P., Kamo, S.L., Allen, C.M., Aleinikoff, J.N., Davis, D.W., Korsch, R.J. & Foudoulis, C. 2003. TEMORA 1: a quality zircon standard for Phanerozoic U-Pb geochronology. *Chemical Geology* **200**, 155–170.

Bonhomme, M.G., Thuizat, R., Pinault, Y., Clauer, N., Wendling, R. & Winkler, R. 1975. *Méthode de datation potassium – argon. Appareillage et Technique (The potassium – argon dating method)*. Notes technique de l'Institut de Géologie, Université Louis Pasteur, Strasbourg **3**.

Boztuğ, D., Erçin, A.İ., Kuruçelik, M.K., Göç, D., Kömür, I. & İskenderoğlu, A. 2006. Geochemical characteristics of the composite Kaçkar batholith generated in a Neo-Tethyan convergence system, eastern Pontides, Turkey. *Journal of Asian Earth Sciences* **27**, 286–302.

Bürküt, Y. 1966. *Kuzeybatı Anadolu'da Yer Alan Plütonların Mukayeseli Jenetik Etüdü [Comparative Genetic Investigation of Northwestern Anatolian Plutons]*. PhD Thesis, İstanbul Technical University [in Turkish with English abstract, unpublished].

Castillo, R.P. 2006. An overview of adakite petrogenesis. *Chinese Science Bulletin* **51**, 257–268.

Castillo, P.R., Janney, P.E. & Solidum, R.U. 1999. Petrology and geochemistry of Camiguin island, southern Philippines: insights to the source of adakites and other lavas in a complex arc setting. *Contributions to Mineralogy and Petrology* **134**, 33–51.

Chen, F., Siebel, W., Satir, M., Terzioğlu, N. & Saka, K. 2002. Geochronology of the Karadere basement (NW Turkey) and implications for the geological evolution of the İstanbul Zone. *International Journal of Earth Sciences* **91**, 469–481.

Chiaradia, M. 2009. Adakite-like magmas from fractional crystallization and melting-assimilation of mafic lower crust (Eocene Macuchi arc, Western Cordillera, Ecuador). *Chemical Geology* **265**, 468–487.

Condie, K.C. 2005. TTGs and adakites: are they both slab melts? *Lithos* **80**, 33–44.

Davies, J.H. & Stevenson, D.J. 1992. Physical model of source region of subduction zone volcanics. *Journal of Geophysical Research* **97**, 2037–2070.

Defant, M.J. & Drummond, M.S. 1990. Derivation of some modern arc magmas by melting of young subducted lithosphere. *Nature* **347**, 662–665.

Defant, M., Richerson, P., De Boer, J., Stewart, R., Maury, R., Bellon, H., Drummond, M. & Feigenson, M. 1991. Dacite genesis via both slab melting and differentiation: petrogenesis of La Yeguada volcanic complex, Panama. *Journal of Petrology* **32**, 1101–1142.

Didier, J. & Barbarin, B. (eds) 1991. *Enclaves and Granite Petrology*. Developments in Petrology **13**, Elsevier, Amsterdam.

Eyüboğlu, Y., Santosh, M. & Chung, S.L. 2011. Crystal fractionation of adakitic magmas in the crust–mantle transition zone: petrology, geochemistry and U–Pb zircon chronology of the Seme adakites, eastern Pontides, NE Turkey. *Lithos* **121**, 151–166.

Hibbard, M.J. 1991. Textural anatomy of twelve magma mixed granitoid systems: *In*: Didier, J. & Barbarin, B. (eds), *Enclaves and Granite Petrology, Development in Petrology* 13, Elsevier, Amsterdam, 431–444.

Hoffmann, A.W. 1997. Mantle geochemistry: the message from oceanic volcanism. *Nature* **385**, 219–229.

Hou, Z.Q., Gao, Y.F., Qu, X.M., Rui, Z.Y. & Mo, X.X. 2004. Origin of adakitic intrusives generated during mid-Miocene east–west extension in southern Tibet. *Earth and Planetary Science Letters* **220**, 139–155.

Kadioğlu, Y.K. & Dilek, Y. 2010. Structure and geochemistry of the adakitic Horoz granitoid, Bolkar Mountains, south-central Turkey, and its tectonomagmatic evolution. *International Geology Review* **52**, 505–535.

Karacik, Z. & Tüysüz. 2010. Petrogenesis of the Late Cretaceous Demirköy igneous complex in NW Turkey: implications for magma genesis in the Strandja Zone. *Lithos* **114**, 369–384.

Karsli, O., Chen, B., Aydin, F. & Şen, C. 2007. Geochemical and Sr-Nd-Pb isotopic compositions of the Eocene Dölek and Sarıçiçek plutons, Eastern Turkey: implications for magma interaction in the genesis of high-K calc-alkaline granitoids in a post-collision extensional setting. *Lithos* **98**, 67–96.

Karsli, O., Dokuz, A., Uysal, İ., Aydin, F., Kandemir, R. & Wijbrans, J. 2010. Generation of the Early Cenozoic adakitic volcanism by partial melting of mafic lower crust, Eastern Turkey: implications for crustal thickening to delamination. *Lithos* **114**, 109–120.

Kay, S.M., Ramos, V.A. & Marquez, M. 1993. Evidence in Cerro-Pampa volcanic-rocks for slab-melting prior to ridge–trench collision in southern South-America. *Journal of Geology* **101**, 703–714.

Keskin, M., Ustaömer, T. & Yeniyol, M. 2003. İstanbul kuzeyinde yüzeylenen Üst Kretase yaşlı volkano-sedimenter birimlerin stratigrafisi, petrolojisi ve tektonik ortamı [Stratigraphy, petrology and tectonic setting of Upper Cretaceous volcano-sedimentary rocks outcropping in the north of İstanbul]. *Proceedings, İstanbul'un Jeolojisi Sempozyumu-I*, 23–35 [in Turkish with English Abstract].

Keskin, M., Ustaömer, T. & Yeniyol, M. 2010. İstanbul kuzeyindeki Üst Kretase volkanojenik istiflerinin magmatik evrimi ve jeodinamik ortamı [Magmatic evolution and geodynamic setting of Upper Cretaceous volcanogenic sequence in north İstanbul]. *Proceedings, İstanbul'un Jeolojisi Sempozyumu III*, 130–180 [in Turkish with English Abstract].

Ketin, İ. 1941. *Alemdağ Batısındaki Granit Masifi Hakkında [About Granite Massif in the West of Alemdağ]*. İstanbul Üniversitesi Jeoloji Enstitüsü Yayını **7**, İstanbul [in Turkish].

Ketin, İ. 1966. Anadolu'nun tektonik birlikleri [Tectonic units of Anatolia]. *Mineral Research and Exploration Institute of Turkey (MTA) Bulletin* **66**, 20–34 [in Turkish].

Ketin, İ. 1983. *Türkiye Jeolojisine Genel Bir Bakış [Geology of Turkey]*. İstanbul Technical University Publications **1259**.

Köksal, S. & Göncüoglu, M.C. 2008. Sr and Nd isotopic characteristics of some S-, I- and A-type granitoids from Central Anatolia. *Turkish Journal of Earth Sciences* **17**, 111–127.

Le Maitre, R. W (Ed.)., Streckeisen, A., Zanettin, B., Le Bas, M. J., Bonin, B., Bateman, P., Bellieni, G., Düdek, A., Efremova, S., Keller, J., Lamere, J., Sabine, P. A., Schmid, R., Sorensen, H. & Woolley, A. R. 2002. *Igneous Rocks*: *A Classification and Glossary of Terms*. Recommendations of the International Union of Geological Sciences, Subcommission of the Systematics of Igneous Rocks. Cambridge University Press.

Lewandowska, A., Banas, M. & Zygon, K. 2007. K-Ar dating of amphiboles from andesite of complex dyke in Dubie (southern Poland). *Geochronometria* **27**, 11–15.

Ludwig, K.R. 2001. *SQUID 1.02, A User's Manual*. Berkeley Geochronology Center Special Publication no. **2**, 2455 Ridge Road, Berkeley, CA 94709, USA.

Ludwig, K.R. 2003. *User's Manual for Isoplot/Ex, Version 3.0, A Geochronological Toolkit for Microsoft Excel*. Berkeley Geochronology Center Special Publication no. **4**, 2455 Ridge Road, Berkeley CA 94709, USA.

Macpherson, C.G., Dreher, S.T. & Thirwall, M.F. 2006. Adakites without slab melting: high pressure differentiation of island arc magma, Mindanao, the Philippines. *Earth Planetary Science Letters* **243**, 581–593.

Maniar, P.D. & Piccoli, P.M. 1989. Tectonic discrimination of granitoids. *Geological Society of America Bulletin* **101**, 635–643.

Martin, H. 1999. Adakitic magmas: modern analogues of Archaean granitoids. *Lithos* **46**, 411–429.

Martin, H., Smith, R.H., Rapp, R., Moyen, J.F. & Champion, D. 2005. An overview of adakite, tonalite-trondhjemite-granodiorite (TTG), and sanitoid: relationships and some implications for crustal evolution. *Lithos* **79**, 1–24.

MTA, 2005. *1:50.000 Ölçekli Türkiye Jeoloji Haritaları* Bursa G22b Paftası *[Turkish Geology Map at 1:50.000 Scale, Bursa G22b Sheet]*. MTA Genel Müdürlüğü, Ankara.

Okay, A.I. & Şahintürk, Ö. 1997. Geology of the Eastern Pontides. *In*: Robinson, A. (ed), *Regional and Petroleum Geology of the Black Sea and Surrounding Regions*. American Association of Petroleum Geologists Memoir **68**, 291–311.

Okay, A.I., Satir, M., Maluski, H., Siyako, M., Monie, P., Metzger, R. & Akyüz, S. 1996. Paleo- and Neo-Tethyan events in northwest Turkey: geological and geochronological constraints. *In*: Yin, A. & Harrison, M. (eds), *Tectonics of Asia*. Cambridge University Press, 420–441.

Okay, A.I., Satir, M., Zattin, M., Cavazza, W. & Topuz, G. 2008. An Oligocene ductile strike-slip shear zone: Uludağ Massif, northwest Turkey – implications for the westward translation of Anatolia. *Geological Society of America Bulletin* **120**, 893–911.

Okay, A.I. & Tüysüz, O. 1999. Tethyan sutures of northern Turkey. *In*: Durand, B., Jolivet, L., Horváth, F. & Séranne, M. (eds), *The Mediterranean Basins: Tertiary Extension within the Alpine Orogen*. Geological Society, London, Special Publications **156**, 475–515.

Öztunali, Ö. & Satir, M. 1973. Çavuşbaşı kristalin karmaşığının petrografi ve petrolojisi [Petrography and petrology of Çavuşbaşı crystalline complex]. *Cumhuriyetin 50. Yılı Yerbilimleri Kongresi*, 445–456 [in Turkish].

Öztunali, Ö. & Satir, M. 1975. Rb and Sr Altersbestımungen an Tıefengesteınen aus Çavuşbaşı (İstanbul). *İstanbul Üniversitesi, Fen Fakültesi Mecmuası* Seri **B 40**, 1–7.

Patiño Douce, A.E. 1999. What do experiments tell us about the relative contributions of crust and mantle to the origin of granitic magmas? *In*: Castro A, Fernandez, C. & Vigneresse, J.L. (eds), *Understanding Granites: Integrating New and Classical Techniques*. Geological Society, London, Special Publications **168**, 55–75.

Pecerillo, A. & Taylor, S.R. 1976. Geochemistry of Eocene calc-alkaline volcanic rocks from Kastamonu area, northern Turkey. *Contributions to Mineralogy and Petrology* **58**, 63–81.

Robertson, A.H.F. & Ustaömer, T. 2004. Tectonic evolution of the Intra-Pontide suture zone in the Armutlu Peninsula, NW Turkey. *Tectonophysics* **381**, 175–209.

Şengör, A.M.C. & Yilmaz, Y. 1981. Tethyan evolution of Turkey: a plate tectonic approach. *Tectonophysics* **181**, 241–981.

Smithies, R.H. & Champion, D.C. 2000. The Archean high-Mg diorite suite: links to tonalite-trondhjemite-granodiorite magmatism and implications for early Archean crustal growth. *Journal of Petrology* **41**, 1653–171.

Smithies, R.H., Champion, D.C. & Cassidy, K.F. 2003. Formation of Earth's early Archean continental crust. *Precambrian Reserach* **127**, 89–101.

Steiger, R.H. & Jäger, E. 1977. Subcommission on geochronology: convention on the use of decay constants in geo- and cosmochronology. *Earth Planetary Science Letters* **36**, 359–362.

Stern, C.R. & Kilian, R. 1996. Role of the subducted slab, mantle wedge and continental crust in the generation of adakites from the Andean Austral Volcanic Zone. *Contributions to Mineralogy and Petrology* **123**, 263–281.

Streckeisen, A. & Le Maitre, R.W. 1979. A chemical approximation to the modal QAPF classification of the igneous rocks. *Neues Jahrbuch für Mineralogie, Abhandlungen* **136**, 169–206.

Sun, S.S. & McDonough, W.E. 1989. Chemical and isotopic systematics of oceanic basalts: implications for mantle composition and processes. *In*: Saunders, A.D. & Norry, M.J. (eds), *Magmatism in the Ocean Basins*. Geological Society, London, Special Publications **118**, 313–345.

Tera, F. & Wasserburg, G. 1972. U-Th-Pb systematics in three Apollo 14 basalts and the problem of initial Pb in lunar rocks. *Earth and Planetary Science Letters* **14**, 281–304.

Topuz, G., Altherr, R., Schwarz, W.H., Siebel, W., Satir, M. & Dokuz, A. 2005. Post-collisional plutonism with adakite-like signatures: the Eocene Saraycık granodiorite (Eastern Pontides, Turkey). *Contributions to Mineralogy and Petrology* **150**, 441–455.

Topuz, G., Okay, A.I., Altherr, R., Satir, M. & Schwarz, W.H. 2008. Late Cretaceous blueschist facies metamorphism in southern Thrace (Turkey) and its geodynamic implications. *Journal of Metamorphic Geology* **26**, 895–913**.**

Topuz, G., Okay, A.I., Altherr, R., Schwarz, W.H., Siebel, W., Zack, T., Satir, M. & Şen, C. 2011. Early Eocene post-collisional adakite-like magmatism in the Ağvanis Massif (Eastern Pontides, Turkey) and implications for the evolution of the Eocene magmatism. *Lithos* **125**, 131–150.

Ustaömer, P.A. & Rogers, G. 1999. The Bolu Massif: remnant of a pre-Early Ordovician active margin in the west Pontides, northern Turkey. *Geological Magazine* **136**, 579–592.

Varol, E., Temel, A., Gourgau, A. & Bellon, H. 2007. Early Miocene 'adakite-like' volcanism in the Balkuyumcu region, central Anatolia, Turkey: petrology and geochemistry. *Journal of Asian Earth Sciences* **30**, 613–628.

Williams, I.S. 1998. U-Th-Pb Geochronology by Ion Microprobe. *In*: McKibben, M.A., Shanks III, W.C. & Ridley, W.I. (eds), *Applications of Microanalytical Techniques to Understanding Mineralizing Processes*. Reviews in Economic Geology **7**, 1–35.

Workman, R.K. & Hart, S.R. 2005. Major and trace element composition of the depleted MORB mantle (DMM). *Earth and Planetary Science Letters* **231**, 53–72.

Yeniyol, M. & Ercan, T. 1989-1990. İstanbul Kuzeyinin jeolojisi, Üst Kretase volkanizmasının petrokimyasal özellikleri ve Pontidler'deki bölgesel dağılımı [Geology of western part of İstanbul, petrochemical properties and regional distrubitions of Upper Cretaceous volcanics]. *İstanbul Üniversitesi, Mühendislik Fakültesi, Yerbilimleri Dergisi* **7**, 125–147 [in Turkish with English Abstract].

Yiğitbaş, E., Elmas, A. & Yilmaz, Y. 1999. Pre-Cenozoic tectono-stratigraphic components of the western Pontides and their geological evolution. *Geological Journal* **34**, 55–74.

Yiğitbaş, E., Kerrich, R., Yilmaz, Y., Elmas, A. & Xie, Q.L. 2004. Characteristics and geochemistry of Precambrian ophiolites and related volcanics from the İstanbul-Zonguldak unit, Northwestern Anatolia, Turkey: following the missing chain of the Precambrian South European suture zone to the east. *Precambrian Research* **132**, 179–206.

Yilmaz, I. 1977. The absolute age and genesis of the Sancaktepe granite (Kocaeli Peninsula)]. *Türkiye Jeoloji Kurumu Bülteni* **20**, 17–20 [in Turkish].

Yilmaz, S. & Boztuğ, D. 1996. Space and time relations of three plutonic phases in the Eastern Pontides, Turkey. *International Geology Review* **38**, 935–956.

Yilmaz, Y., Genç, S.C., Yiğitbaş, E. Bozcu, M. & Yilmaz, K. 1995. Geological evolution of the late Mesozoic continental margin, Northwestern Anatolia. *Tectonophysics* **243**, 155–171.

Yilmaz, Y., Tüysüz, O., Yiğitbaş, E. Genç, Ş.C & Şengör, A.M.C. 1997. Geology and tectonic evolution of the Pontides. *In*: Robinson, A.G. (ed), *Regional and Petroleum Geology of the Black Sea and Surrounding Region*. AAPG Memoir **68**, 183–226.

Yilmaz-Şahin, S. 2005. Transition from arc- to post-collision extensional setting revealed by K-Ar dating and petrology: an example from the granitoids of the Eastern Pontide Igneous Terrane, Araklı-Trabzon, NE Turkey: *Geological Journal* **40**, 425–440.

Yilmaz Şahin, S., Güngör, Y. & Aysal, N. 2010. İstanbul'un granitoyidleri (Granitoids of İstanbul]. *Proceedings, İstanbul'un Jeolojisi Sempozyumu III*, 100–129 [in Turkish with English Abstract].

Yilmaz Şahin, S., Güngör, Y., Aysal, N. & Öngen, S. 2009. Istranca ve İstanbul zonları (KB Türkiye) içerisinde yüzeylenen granitoyidlerin jeokimyası ve SHRIMP zirkon U-Pb yaşlandırması [Geochemistry and SHRIMP zircon U-Pb dating of granitoids outcropping in the Strandja and İstanbul zones (NW Turkey)]. *Abstracts, 62. Türkiye Jeoloji Kurultayı* [in Turkish].

Yilmaz Şahin, S., Güngör, Y. & Boztuğ, D. 2004. Comparative petrogenetic investigation of composite Kaçkar batholith granitoids in eastern Pontide magmatic arc-northern Turkey: *Earth, Planets, Space* **56**, 429–446.